SPIE Symposium: X-Ray Mirrors and Crystals III (AM302), 7–11 July 2002, Seattle, USA

The toroidal mirror for single-pulse experiments on ID09B

L. Eybert, M. Wulff, W. Reichenbach, A. Plech, F. Schotte, E. Gagliardini, L. Zhang,

O. Hignette, A. Rommeveaux and A. Freund

European Synchrotron Radiation Facility, B.P. 220, F-38043 Grenoble France

ABSTRACT

ID09 is a dual-purpose beamline dedicated to time-resolved and high-pressure experiments. The time-resolved experiments use a high-speed chopper to isolate single pulses of x-rays. The chopper is installed near the sample (focal spot) and the shortest usable opening time depends on the sharpness of the vertical focus. In the 16-bunch mode, the opening window of the chopper has to be reduced to 0.300 μs to select single pulses of x-rays. This can only be achieved by reducing the height of the tunnel in the chopper to 0.143 mm. To ensure a reasonable transmission though the tunnel, we have built a very precise toroidal mirror that focuses the beam 22.4 m downstream with a defocusing parameter M= 0.677. The 1.0-m long silicon mirror is curved by gravity into a near perfect toroid with a meridional radius of 9.9 km. The curvature is fine-tuned by a stepper motor that pushes from below. The combined figure error from the gravity sag and the corrective force is less than 0.3 μrad. The polishing error is 0.7 μrad (rms) averaged over the central 450-mm of the 1000 mm long mirror. The measured size of the polychromatic focus is 0.100 x 0.070 mmh x mmv, which is in agreement with the prediction from the Long-Trace-Profiler (LPT) at the ESRF. The small focus, which integrates the full central cone of the U17 undulator, is the result of superb optical quality, fine-control of curvature, strain-free mount, a vibration free cooling system and careful alignment.

1. INTRODUCTION

Beamline ID09B at the European Synchrotron Radiation Facility is dedicated to time-resolved pump and probe experiments on photosensitive molecules. A comprehensive set-up is available for studies of chemical or bio-chemical reactions triggered by femtosecond and nanosecond laser pulses. The structural changes are probed by delayed x-ray pulses from single bunches of electrons. In experiments triggered by the femtosecond laser, the time-resolution can be pushed to the 50-200 ps bunch limit (fwhm), the ultimate time-resolution for pump and probe experiments on a synchrotron. Our experimental program includes Laue diffraction on macromolecules, small-molecule diffraction, powder diffraction and diffuse scattering from liquids. A recent review of these experiments can be found in [1] and examples of our experiments can be found in[2-5]

The success of a pump and probe experiment depends on the quality of the laser excitation and the quality of the-ray beam. Concerning the latter, the key parameter is the number of photons that can be focused on the sample in a single pulse. The second key parameter is the frequency at which the excitation can run. Heatload from the laser (crystals), finite injection speed of the sample (liquids), and of course, the time scale of the phenomenon itself, typically reduce the usable excitation frequency to 1-1000 Hz. This is far below the frequency of the synchrotron that runs between 0.354 to 352 MHz. This dramatic mismatch makes these experiments demanding and only optimized undulator beamlines can undertake such studies. The most important development in the last few years has been the introduction of single-harmonic undulators with narrow bandwidths (3%) that can deliver about 1000 times more photons on the sample as compared to a conventional monochromatic beam. In this paper we describe a second-generation toroidal mirror. Its prime function is to focus and reject higher harmonics from the monochromatic or pink beam.

2. THE INSERTION DEVICES

For us the optimal undulator configuration is to have two in-vacuum undulators in the straight section: a low-K undulator for high-flux experiments in a narrow energy range combined with a higher-K undulator with complete tunability. Our new undulator, the U17, has a 17-mm magnetic period, a K of 0.86. The fundamental energy is 14.8 keV at 6.0 mm gap and this energy can be varied from 14.8 to 20.4 keV. The calculated polychromatic spectrum is shown in figure 1and the source parameters are listed in table 1. The main virtue of this undulator is its high flux on the fundamental: it produces 1.1 x 10^{10} photons in a 3.2% bandwidth around 14.8 keV in *one* pulse (10mA mode). The efficiency of this undulator is due to a good match between the critical energy of the individual bends in the sinusoidal orbit, 13.2 keV, and the undulator fundamental at 14.8 keV. Consequently the radiation is predominantly loaded into the first harmonic. We consider 15 keV the *golden energy* for diffraction experiments since numerous Laue experiments on proteins have shown this energy to give the highest number of diffracted to absorbed photons. That optimizes the lifetime and the information yield.
The total power of the 2.0 m long undulator is 2740 W of which 450 W lies in the central cone. The U17 is particularly good for Laue diffraction of macromolecules (ref) but it is also very nice for diffuse scattering experiments from liquids where it is operated at slightly opened gap in order to reduce the second harmonic.

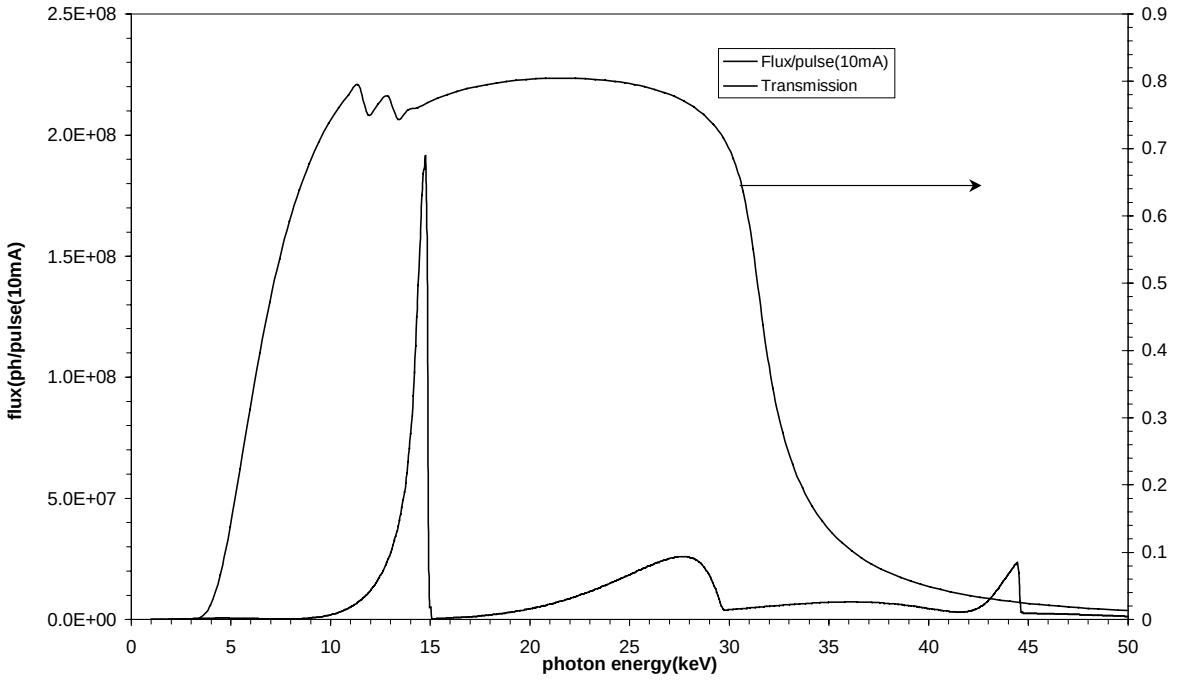

Figure 1. Polychromatic spectrum of the U17 undulator from a single bunch of electrons (10 mA single bunch mode, 28.2 nC per bunch). The calculated transmission of the front-end, the beryllium window and the toroidal mirror (Pt coated at 2.722 mrad) is shown on the right.

Table 1. Source parameters for the U17 and U46 undulators. The source size (fwhm) is 0.117 mm horizontally and 0.024 mm vertically for the low-beta site on ID09. The power density in the center of the central cone of the U17 is 95 W/mm^2 (200mA).

Period(mm)	poles	minimum gap (mm)	Bmax(T)	E_f(keV)	E_c(keV)	K	P(W/200 mA)
17	235	6.0	0.544	14.84	13.2	0.86	2740
46	71	16.0	0.643	0.64	15.6	2.76	3116

3. THE OPTICAL LAYOUT

In our new second-generation layout, the first optical element in the beamline is a cryogenic channel-cut monochromator based on a monolithic silicon (111) crystal. The energy can be varied between 4-50 keV and the (orthogonal) distance between the two crystals is 4.0 mm. The monochromator is cooled from the sides and rocking curve tests have shown that the performance is near perfect up to 450-Watt[6]. The monochromator vessel is mounted on a lateral translation stage, which in the future will allow us to insert a cryogenically cooled multilayer system. The second optical element is a platinum coated toroidal mirror. It is located 33.1 m from the source and it works at a fixed angle of 2.772 mrad. The mirror focuses the radiation 22.4 m downstream (M= 0.677). The layout of the optics hutch is shown in figure 2. Note the so-called heatload shutter upstream the monochromator. It gates the toroidal mirror from the continuous heatload from the (closed gap) undulator. It is designed to produce 20 ms bursts of white beam at a frequency up to 5 Hz. It is synchronized with the millisecond shutter and the chopper that are located just in front of the sample. As a typical Laue diffraction experiment is repeated at 3 Hz, the heatload shutter reduces the heatload on the mirror to 6%. That improves the stability and sharpness of the focus substantially and ensures that the focused beam is always centered in the tunnel of the chopper.

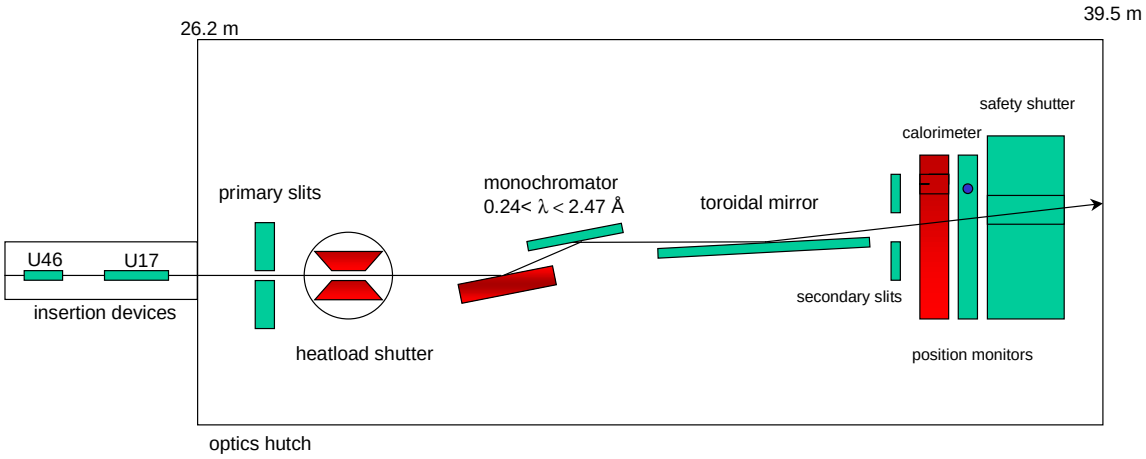

Figure 2. The optics hutch components on ID09B.

4. THE CHOPPER

The function of the chopper is to select single pulses of x-rays from the 1-bunch, 16-bunch and hybrid mode of operation. It rotates at 896.6 Hz, the 396th sub-harmonic of the ring frequency and selects one pulse every 1.11 ms. Likewise, the femtosecond laser is running at 896.6 Hz and their relative timing is set electronically by delaying or advancing the laser. The chopper wheel consists of a flat triangular rotor that rotates about a horizontal axis perpendicular to the x-ray beam. The 165-mm long tunnel is located on one side of the triangle. The tunnel is 4.0 mm wide and its height varies from 0.9 mm at one wall to 0.050 mm at the other wall, i.e. the cross section of the tunnel is trapezoidal. By displacing the chopper laterally, the opening time can be varies from 0.105 μs to 1.892 μs. In the 16-bunch mode, the pulses are 0.176 μs apart and the opening window should be smaller that twice 2 x 0.176 μs = 0.352 μs. As the chopper rotates with a 10 ns(rms) jitter, we are forced to reduce the opening time to about 0.300 μs to avoid (partial) double pulses. That corresponds to a tunnel height of 0.143 mm. The vertical focal size should match that to ensure high transmission in the 16-bunch mode. Neglecting spherical aberrations, which are very small in the present configuration, the vertical focal size is dominated by the slope error of the mirror. It can be approximated by:

$$F_z = \left\{ (M\,Sz)^2 + (2\,q\,\alpha)^2 \right\}^{1/2}$$

Here S_z is the electron source size, M the demagnifying factor, α the slope error and q the distance between the mirror and the focus. The calculated vertical focus is shown in figure 3 together with the acceptance though a 0.143-mm aperture (y-scale on the right). Note that a 1.0 μrad error leads to a 0.105-mm vertical focus with 93% transmission though the 16-bunch tunnel.

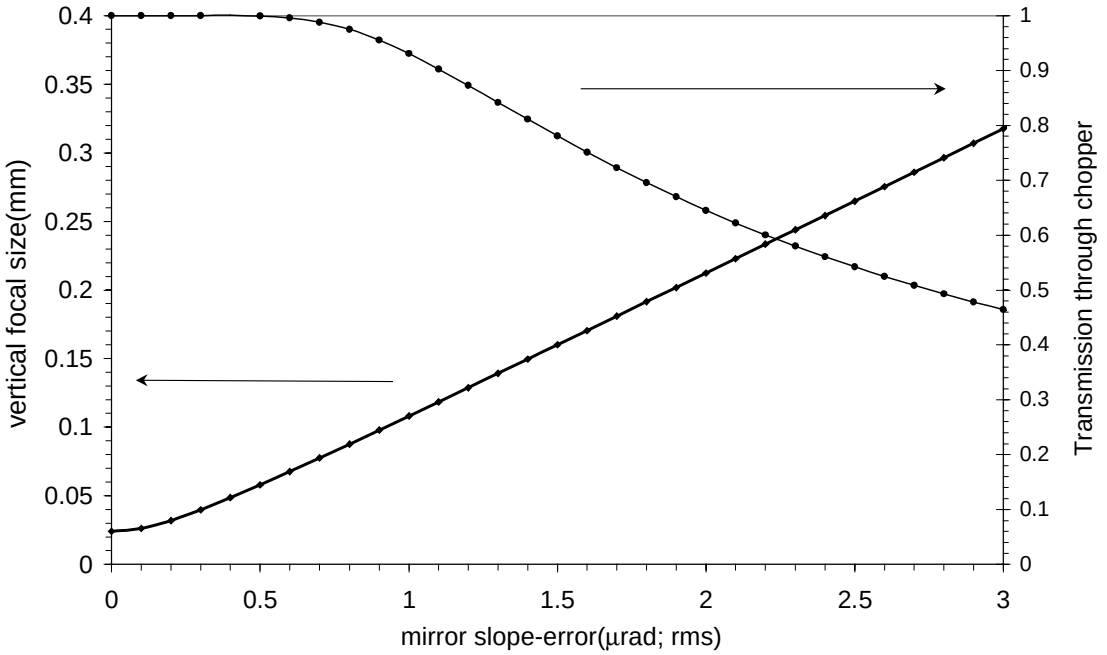

Figure 3. The vertical focal size as a function of slope-error of the toroidal mirror. The focal spot is 22.4 m from the mirror. The scale on the right shows the transmission through a 0.143-mm vertical aperture, the chopper channel used in the 16-bunch mode.

5. THE TOROIDAL MIRROR

In the initial layout of the beamline, the toroidal mirror was the first optical element. It was continuously illuminated by the white beam and the varying heatload lead to drifts of the focus. This problem is now solved by the use of a heatload shutter (white beam mode) and placing the cryogenically cooled monochromator first in the beamline (monochromatic mode). The platinum-coated mirror receives the beam at 2.722 mrad, and reflects between 0-30 keV. The mirror is 33.1 m from the source and focuses 22.4 m downstream (M=0.677). The sagittal and meridional radii are 71.6 mm and 9.95 km respectively.

a) The Mechanical Design

As the meridional radius is fixed (9.95 km) and relatively high, we have built a very simple mechanical bender with the aim to minimize the figure error in the central 450 mm long part of the mirror which is effectively illuminated at 2.722 mrad incidence.

Due to recent improvements in mirror polishing and metrology, it is now possible to produce mirrors of outstanding optical quality. In the call for tender, we therefore specified the longitudinal slope-error to be less than 0.7 μrad (rms) in the 450-mm central zone. With an optical quality of this caliber, is becomes increasingly important to hold, cool and bend the mirror in a controlled manner. Note that in the absence of vibrations, the vertical focus should thus be as small as 75 μm (fwhm). The mirror is supported at each end and we use the gravity sag on the central part to bend the mirror. At one end, the mirror rests on one point (a ball between two conical mechanical parts in order to have a reference for positioning). This ball is preloaded with mechanical springs. That keeps the ball in the cones, which increases the mechanical

stiffness and the vibrational behavior. At the other end, two cylinders are mounted perpendicular to the length of the mirror. These “wheels” allow the mirror to slide longitudinally, which relieves the stress from the bending and the expansion & contraction stress from the bake-out. In order to adjust the curvature, a central stepper motor pushes from below the mirror through a spring and fine tunes the curvature.

b) Cooling System.

The mirror is cooling system are thus eliminated. As the efficiency of the cooling is depends on the filling of the InGa channels, the absorbers can be inserted and extracted from the channels to make the introduction (or extraction) of the InGa easier. See figure 5 and 6.loaded with 450 Watt of beam of which 110 Watt is absorbed. The heat is extracted laterally by cooling copper plates that are dipped into indium gallium filled channels (2*50 cm^3). Stress and vibrations from the

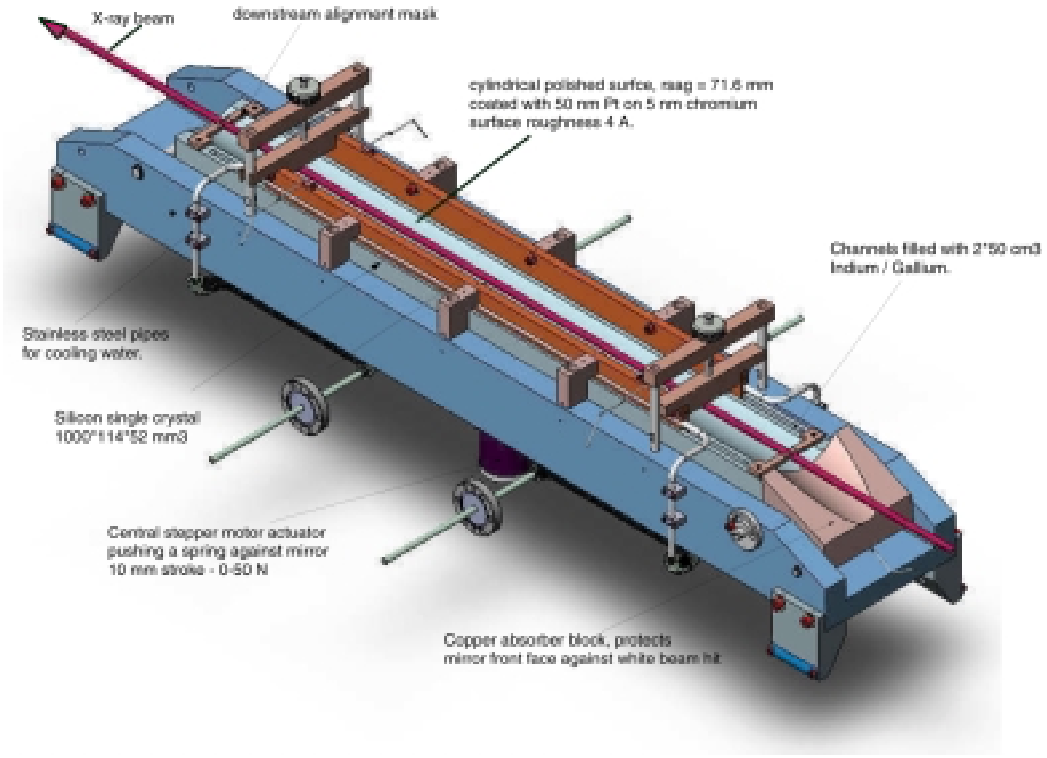

Figure 5. Mechanical design of the mirror holder

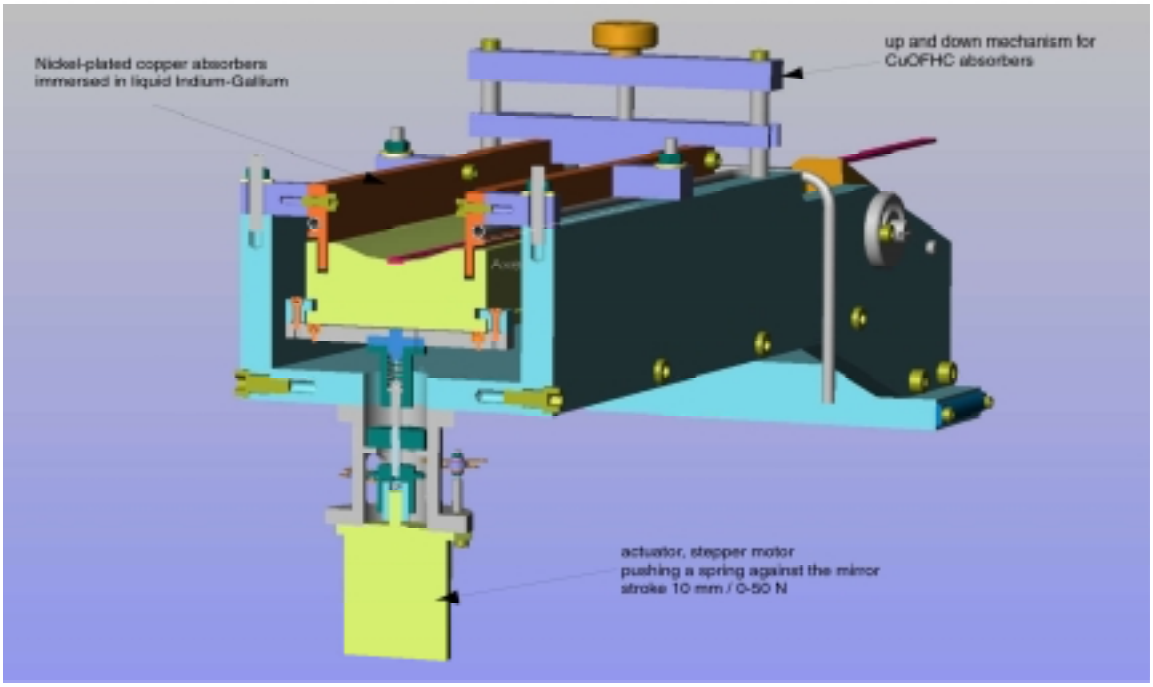

Figure 6. The central actuator and the cooling system

c) FEA calculations and results

In order to predict for the real geometry of the mirror (toroidal shape and cooling channels) and the load of indium gallium coolant, the slope-errors have been calculated by FEA (Finite Element Analysis). It permits, for a given geometry, to examine how gravity and the central force change the shape of the mirror. The thickness of the mirror, which control the inertia and the characteristics of the central actuator (stroke, resolution and stiffness of the spring) was optimized.
It's important to note that initial shape of the mirror has to be included in the calculations. Actually the meridional radius of the mirror, measured without gravity, was not considered flat ($R_0=\infty$). The reason is that it is very difficult to polish a mirror to a specific meridional radius (9.95 km for example) whereas it is relatively easy to get a mirror with a larger meridional radius between 25 km to ∞.

Table 2- Mirror parameters.

shape :	cylindrical(in gravity -> toroidal)
dimensions : L x W x H(mm^3)	1000 x 114 x 52
material	silicon - E = $130*10^9$ Pa ρ_{si} = 2340 kg/m^3
sagittal radius(mm)	71.6
coating	Pt – 40 nm
surface roughness(Å; rms)	1.3
incidence angles (mrad)	2.722
energy range(keV)	4-34
P = source-mirror distance(m)	33.05
Q = mirror-focus distance(m)	22.37
Demagnification M	0.677
slope-error(µrad; rms) – 450 mm	0.7 µrad
residual meridional radius(km) (no gravity)	[∞ to 25.0]
gravity curvature(km)	9.9

Cooling channels	Length 940 mm Width 7 mm Depth 20 mm Vol. In. Ga. 100 cm^3 ρ_{InGa} 6240 kg/m^3
Mechanical bender	Distance between support 900 mm. (each support at 50 mm from the end of the mirror).
Central actuator	Stroke 10 mm Resolution 0.05 N (roughly 10 m in meridional radius). Upward trust 0-50 N

FEA Results:

$R_{desired}$ = 9.95 km			
R_0	∞	25	km
R_{mean} gravity	9.94	16.5	km
$F_{actuator}$	0.398	27.238	N
R_{mean} gravity + $F_{actuator}$	9.95	9.95	N
Slope error $\Delta\theta_{rms}$ (500 central mm)	0.83	0.15	µrad

Discussion:

The thickness of the mirror (52-mm) and the distance between the supports (900-mm) have been chosen such that the central actuator has to push upward (simplicity of the actuator and lower slope error due to gravity compensation).
The best results have been obtained for a residual curvature R_0 = 25 km. Figure 7 and 8 show that gravity introduces some slope errors (it's why that most mechanical benders use mechanical pusher springs in order to first compensate the gravity). For R_0 = 25 km, these errors are almost completely eliminated with an actuator force of Fc = 27N. Thus the residual slope error is low and acceptable (0.15 µrad), in the central area (-250 / +250 mm).
In the case of R_0 = ∞, gravity can not be compensated because Fc ≈ 0 N. The residual slope error is high and unacceptable (0.83 µrad). But according to mirrors manufacturers, the probability of having a flat mirror is negligible (polish process). In this extreme case, one would have to increase the distance between the supports from 900mm to the maximal distance (almost 1000-mm). The slope error will then attain a reasonable value (< 0.3 µrad in the central zone).

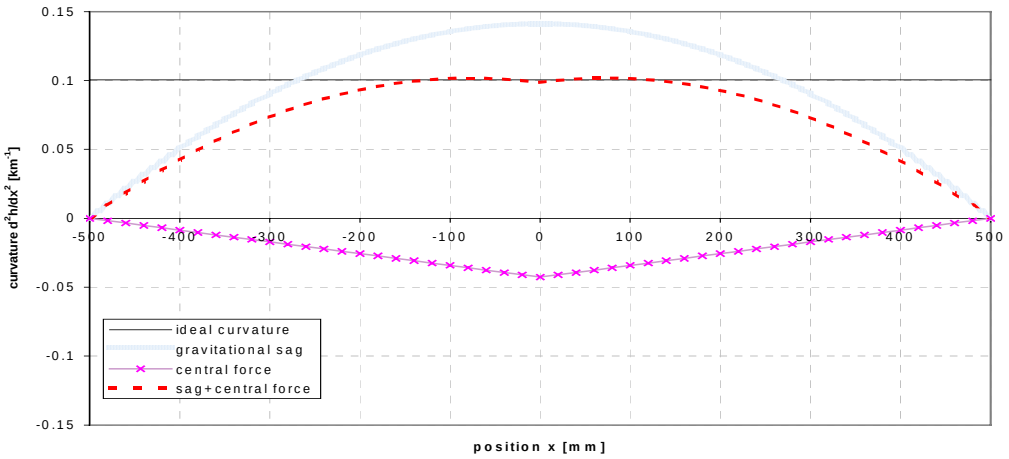

Figure 7. Curvatures (1/R)
The central actuator is used to adjust the meridional radius to 9.95 km and to compensate a part of slope errors introduced by the gravity sag.

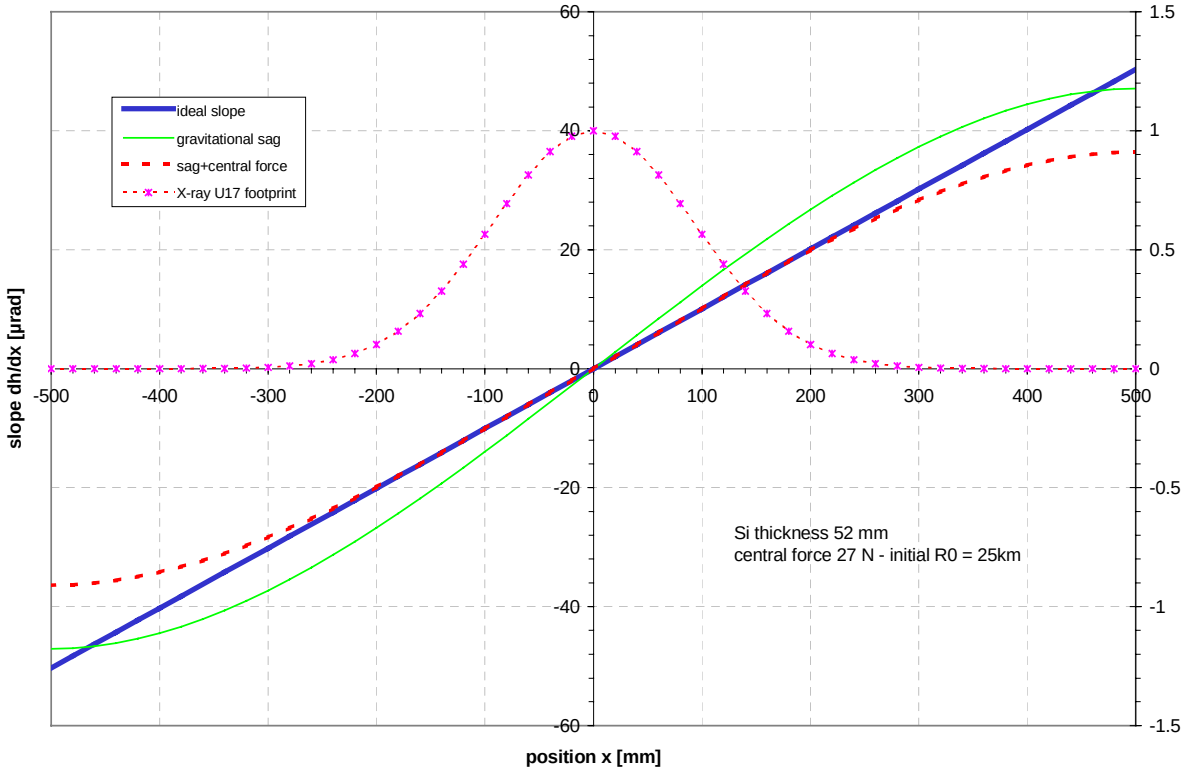

Figure 8- slopes

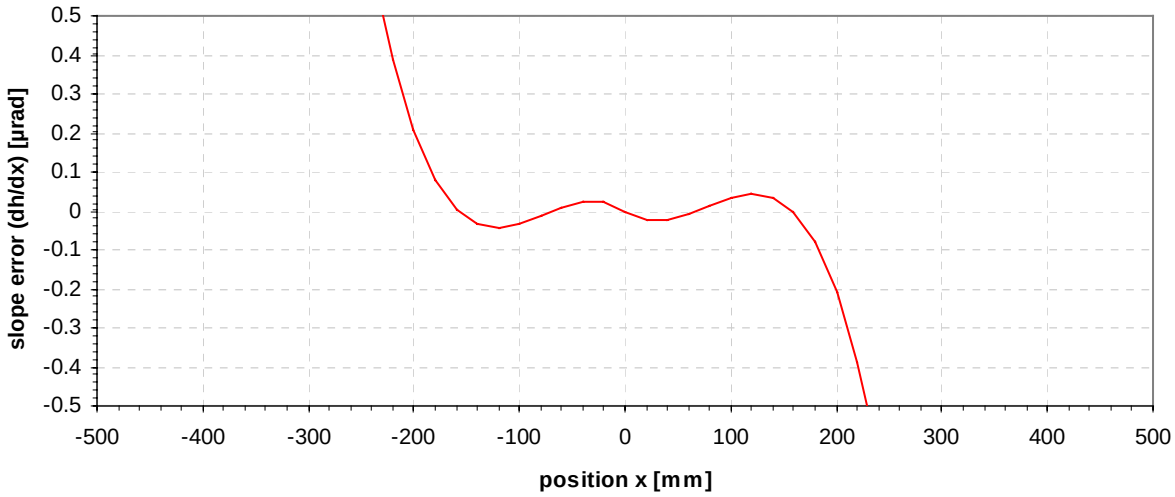

Figure 9. The slope error weighted by intensity from U17 ondulator footprint distribution is less than 0.1 µrad in the zone –250 to + 250 mm.

d) LTP results.

The radius of curvature, slope errors, profile and shape errors of the mirror, which was made by SESO (Société Européenne de Systemes Optiques) have been measured at ESRF on a Long Trace Profiler (LTP).

	Measured length (mm)	Gravity removed	Actuator displacement (mm)	Radius of curvature (km)	Slope error RMS (μrad)
Mirror alone	450	yes	/	28	0.7
Mirror + bender	450	no	0	7.6	1
Mirror + bender	450	no	4	8.9	0.8
Mirror + bender	450	no	5	9.6	0.8
Mirror + bender	450	no	6	10.1	0.8

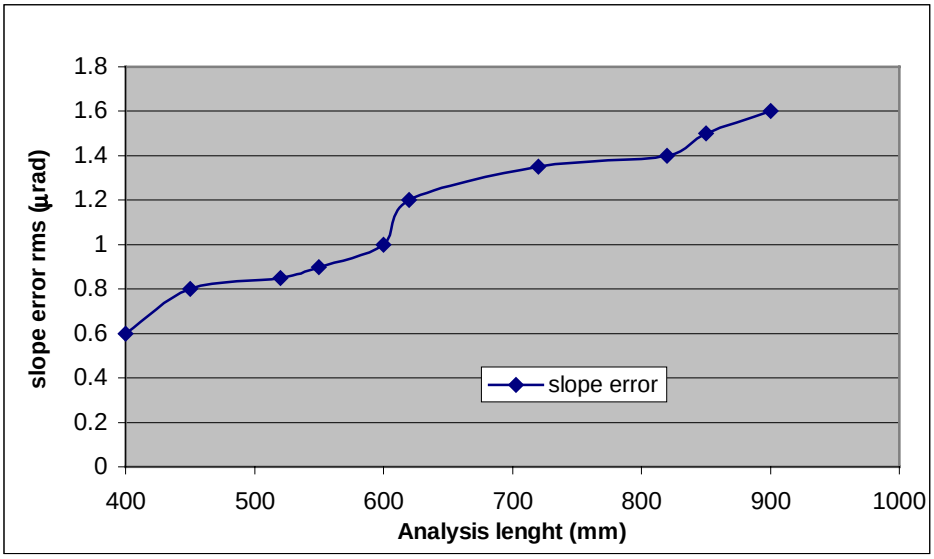

Figure 10. The LTP measured slope-error along the length of the mirror

The measurements obtained with the LTP confirms the FEA results:

- The initial mirror shape error is conserved after mounting the mirror in the bender.
- When the actuator pushes the mirror (to adjust the meridional radius), part of slope error due to the gravity is eliminated and slope error is improving.
- Figure 9 shows that slope error is very low (<1 μrad) in the central 600 mm

6. Experimental Results

As the sharpness of the focus depends critically on the alignment of the mirror, we will briefly describe our alignment method, which will be computerized in the future. The first step is to define the *central ray* in the beamline. The best approach is to load a small white beam on the monochromator and monitor the monochromatic intensity on a PIN diode. The energy of the monochromator is scanned and the monochromator moved to the top of the first harmonic (or odd harmonic). Then we define a small 0.05-mm vertical beam (or gap) on the primary slits and scan its vertical offset. The scan gives the vertical position of the central cone. A similar procedure gives the horizontal center. The primary slits are now calibrated on the central cone (and not the polychromatic beam which is contaminated by the up-stream and down-stream bending magnets).
The toroidal mirror is aligned from the shadow it casts on the PIN diode in the white beam. The best result is obtained by having a pair of slits downstream the mirror to prevent reflections from hitting the diode. The mirror position and angle is controlled by four jacks, two vertical and two horizontal. The prealigned mirror is first moved upwards and parked in the 50% transmission point. The incidence angle is then scanned and

moved to the maximum transmission point. The mirror height is then scanned again and moved to the 50% point. The horizontal alignment is critical. The mirror is first scanned horizontally and moved to maximum transmission. In the next step, the mirror is inclined –0.5 mrad, then scanned vertically and parked at the 50% point. The white beam is now at the bottom of the upstream cylindrical cut; the down stream cut is out of the beam. The position of the upstream horizontal translation is now scanned and positioned at maximum transmission. The down stream horizontal translation is scanned similarly at 0.5 mrad incidence. In this way the two horizontal translations are centered.

The reflectivity of the mirror was studied using energy scans of the undulator spectrum in the direct and reflected beam. A 7.25 x 0.67 mm^2 beam white beam (the central cone) was loaded on the monochromator and the monochromatic intensity recorded on the PIN diode at the end of the optics hutch. The slits in front of the diode were set to only accept the beam from the mirror. The procedure was repeated with the mirror at 2.722 mrad. The ratio is the reflectivity. The absolute flux of both beams is shown in figure 11 and the reflectivity is shown on the scale on the right. The main finding is that the energy cut-off is 4 keV lower than expected. This may be explained by assuming that the density of platinum is lower than the bulk density. Comparisons with reflectivity code XOP indicate that the density is 79 % of bulk platinum. We are currently investigation whether the mirror should be recoated.
Finally the focal spot was optimized in two steps. First the incidence angle was fine-tuned by measuring the horizontal focal size for ten incidence angles around the nominal incidence angle. Then the vertical focal size was fine tuned scanning the stepper motor below the mirror that controls the curvature. The contour plots in figure 12 show the result for the poly and monochromatic beam. The polychromatic focus is 0.100 mmh x 0.070 mmv.

Figure 11. The measured spectrum (or flux) of the U17 undulator at 6.6 mm gap. The spectrum has been measured with

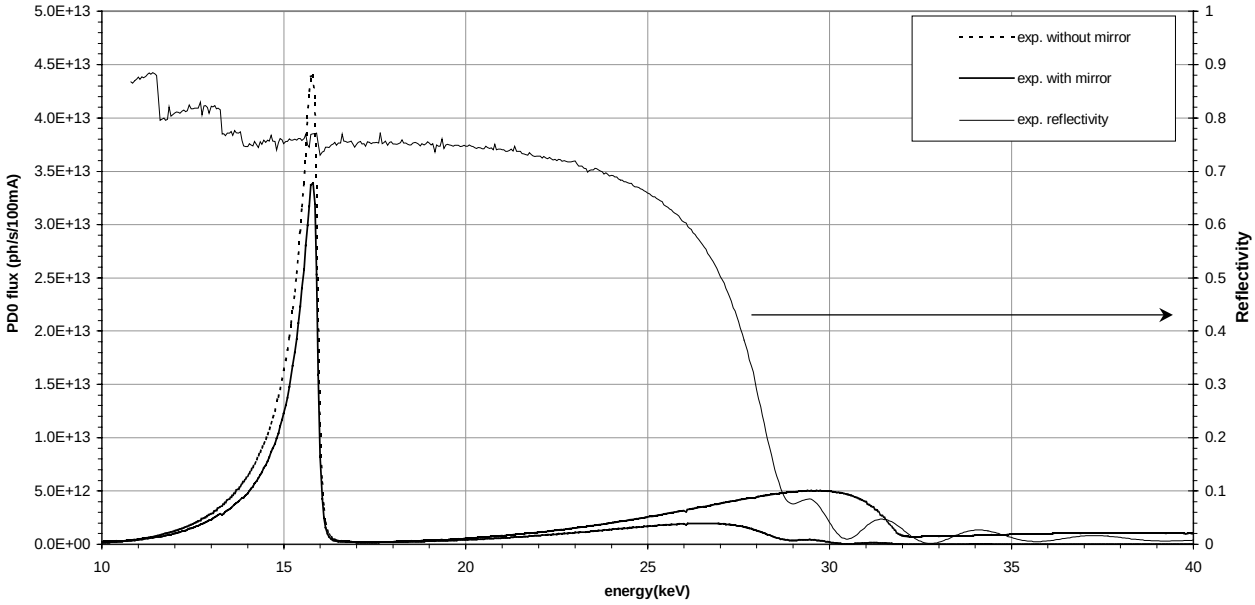

and without toroidal mirror. The reflectivity is shown on the right. The oscillations at high energies are due to the finite thickness for the Pt layer. It is found to be 400 Å thick.

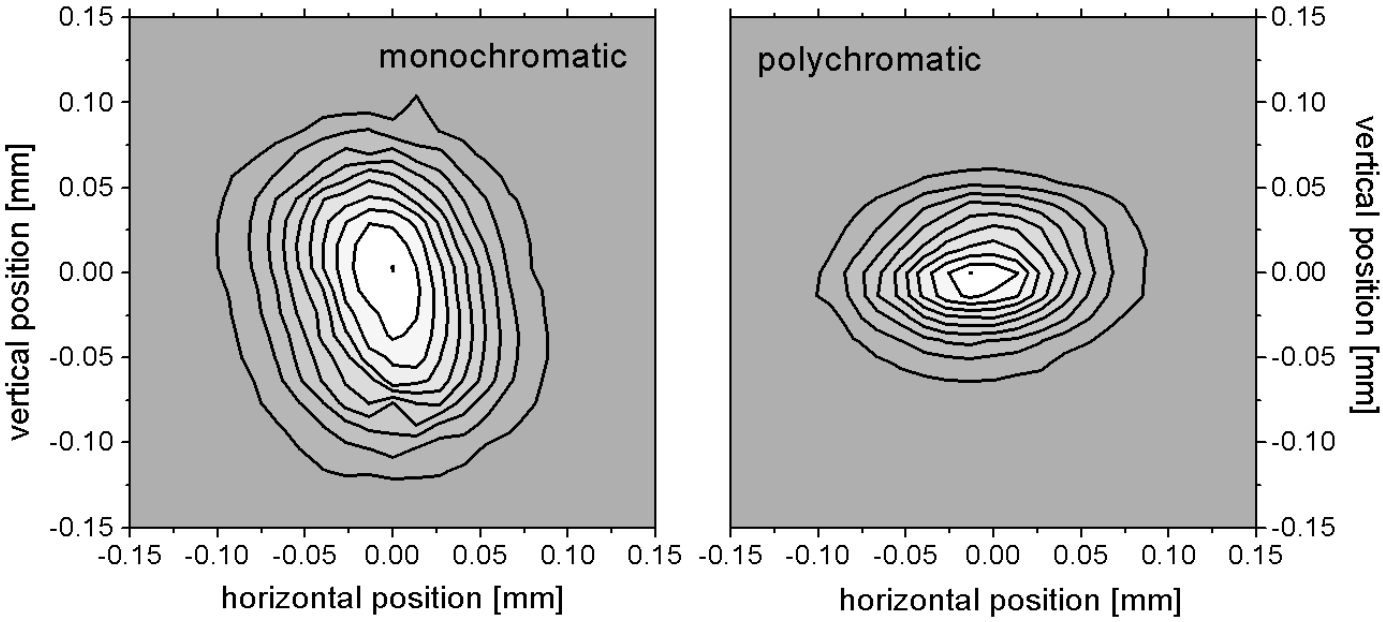

Figure 12. Contour plots of the mono and polychromatic focus of the U17 undulator. The monochromatic focus is broader that the polychromatic due to a very slight (thermal) slope error on the first crystal in the monochromator.

6. Conclusion and outlook

The optical finish of synchrotron mirrors have improved very substantially due to advances in machining ,polishing techniques and metrology for shape and roughness analysis. For example the first toroidal mirror on ID09, delivered in 1993, had a slope error of 4.3 μrad (rms) as compared the new one at 0.7 μrad (rms). The gain in flux for time-resolved experiments is roughly the ratio of the two, which gives a six-fold increase in the flux on the sample in the 16-bunch mode. In addition, new single-harmonic undulators have increased the flux by 5-10. This enormous increase in flux for pump and probe experiments has recently been used in experiments on the recombination of iodine atoms to form the I_2 molecule in the CCl_4 solvent. The new flux values are summarized in table 3. Note for example that a pink beam from the U17 undulator running at 896.6 Hz has the intensity of a classical undulator beam with a Si (111) monochromator. The increase in flux is not only giving better data for of known phenomena, it will enable new discoveries to be made in the near future. We hope that our technical & scientific developments at the ESRF will lay the practical foundation for future femtosecond experiments with a Free Electron Laser.

Table 3. Flux numbers for single-shot and stroboscopic experiments in single bunch mode (10 mA; U17).

Beamline configuration	Single-shot flux (ph/10-mA pulse)	Flux at 896.6 Hz (ph/s/10mA)
Focused monochromatic at 14.8 keV	2.4×10^{7}	2.2×10^{10}
Focused multilayer	1.7×10^{9}	1.5×10^{12}
Focused polychromatic	1.1×10^{10}	9.6×10^{12}

Acknowledgment

The authors are thankful for discussions with Wilfried Schildkamp and J. F. Fermé.

References

1. Schotte, F., *et al.*, *Recent Advances in the Generation of Pulsed Synchrotron Radiation Suitable for Picosecond Time-resolved X-ray Studies.* Third-Generation Hard X-ray Synchrotron Radiation Sources, Edited by Dennis Mills, John Wiley & Sons, Inc, 2002(ISBN 0-471-31433-1): p. 345-401.
2. Srajer, V., *et al.*, *Photolysis of the carbon monoxide complex of myoglobin: nanosecond time- resolved crystallography.* Science, 1996. **274**(5293): p. 1726-9.
3. Perman, B., *et al.*, *Energy transduction on the nanosecond time scale: early structural events in a xanthopsin photocycle.* Science, 1998. **279**(5358): p. 1946-50.
4. Techert, S., F. Schotte, and M. Wulff, *Picosecond X-ray Diffraction Probed Transient Structural Changes in Organic Solids.* Phys. Rev. Lett., 2001. **86**(10): p. 2030-2033.
5. Neutze, R., *et al.*, *Visualizing photochemical in solution though picosecond X-ray scattering.* Phys. Rev. Lett., 2001. **87**(no 19): p. 195508-1 to 195508-4.
6. Zhang, L., *et al.*, *FEA predicted thermal slope errors and comparison with measured rocking curve widths.* SPIE Symposium: X-Ray Mirrors and Crystals III (AM302), 7-11 July 2002, Seattle, USA, 2002.